CLM - P 519

CLM - P 519

UKAEA

Preprint

SPECTROSCOPY OF HIGH DENSITY PLASMAS

N J PEACOCK

CULHAM LABORATORY
Abingdon Oxfordshire

1978

CLM-P 519

SPECTROSCOPY OF HIGH DENSITY PLASMAS

N J Peacock

Culham Laboratory, Abingdon, Oxon, OX14 3DB, UK,
(Euratom/UKAEA Fusion Association)

ABSTRACT

This paper deals with the effects of high density on measurable quantities, such as line shapes and level populations, which may be used to derive plasma parameters in mainly highly-ionised plasmas. The discussion is centred around plasmas with electron density above 10^{18} cm^{-3} and includes vacuum spark plasmas, laser-irradiated solid targets and the plasma focus. These sources have in common a high kinetic energy concentration and are capable of producing the most highly-ionised atomic species observed in the laboratory.

Some of the more topical spectroscopic aspects of high density plasmas are discussed, including interpretation of satellite line features; the effect of correlations and screening on line shapes; opacity as a diagnostic for streaming motion and amplification of XUV line intensities by stimulated emission.

(Paper to be published in Proceedings of the 13th International Conference on Phenomena in Ionized Gases, Berlin, 12-17 September 1977.)

December 1977

INTRODUCTION

Our understanding of the physics of high temperature laboratory plasmas has been greatly assisted in recent years by the accuracy of laser beam scattering techniques in determining plasma parameters. At very high density, however, laser probes cease to be effective due to absorption and refraction of the light beam and one has then to rely on 'classical' methods of analysis, particularly on emission spectroscopy. These dense plasma sources, where emission spectroscopy still plays a unique role, include pinch devices such as the 'plasma focus' [1] [2] the low-inductance vacuum spark [3] [4] [5] and those plasmas created by irradiation of solids with powerful beams of electrons or photons. In recent laser beam interaction experiments with solid targets, electron densities as high as those in the solid state have been deduced [6] while proposals for reaching several orders of magnitude above solid state densities are being pursued in laser driven thermonuclear fusion research [7].

While their intense luminosity, particularly in the x-ray region of the spectrum, make these plasmas easy to observe, spectroscopic studies are inherently difficult due to short plasma sustainment times ($\lesssim$ nanoseconds) steep density and temperature gradients and often appreciable optical opacity. The effects of a high density plasma environment on the emission from atomic systems are twofold. Firstly, collisional rate processes can dominate over radiative rates at least for transitions in or near the visible region. Binary scaling of rate processes [8] using reduced parameters for temperatures, $\Theta = T_e/z^2$ and density $\eta \propto n_e/z^7$ and population of levels $\eta(p) = \frac{n_e}{n(z)Z}\, n(p)$, may become inappropriate at the highest range of densities ($\sim 10^{24}$ cm^{-3}) considered in

this paper. Ground level populations may no longer be considered much longer-lived than the excited level life times in ions of low charge state.

The second effect is due to the plasma microfield on the shift and broadening of atomic energy levels and on the depression of the ionisation potential. Screening of the ion microfield by the electrons becomes important when the number of ions per debye sphere is reduced to the order of unity or less at high density. Non-linear coupling of plasma waves to the atomic systems can also affect the spectral line emission even in quiescent plasma conditions at high densities. While some of these topics are treated in review articles on plasma spectroscopy [9] [10] [11] perhaps only Vinogradov et al, (1974) [12] exclusively deals with high density effects.

Several topics of spectroscopy, mainly of highly-ionised matter in high density plasmas, are treated in this paper. The effects of very high density are dealt with initially in general terms. This is followed by specific descriptions of satellites, line broadening and opacity. Finally, in section 7, level populations are discussed.
We choose to ignore the intensive current effort on atomic term structure of highly-stripped ions since this has a zero-order dependence on the plasma parameters.

2. LIMITATIONS TO LASER PROBE DIAGNOSTICS AT HIGH DENSITIES

Before discussing emission spectroscopy at very high densities, it is worthwhile recalling the limitations to diagnostics based on probe light beams. The 'cut-off' density at which a laser of wavelength λ_o will cease to propagate through the plasma is given by

$$\lambda_c^2 \, n_{ec} = 1.12 \times 10^{13} \cdot \mathrm{cm}^{-1} \qquad \ldots (1)$$

corresponding to densities $n_{ec} \sim 5 \times 10^{21}$ cm^{-3} for visible lasers. In order to avoid severe absorption it is advisable to have a density not more than about $n_{ec}/3$. While successful interferometry of the 'plasma focus' has been made at $n_e \simeq 5 \times 10^{19}$ cm^{-3} [2] there is some loss of resolution due to refraction and plasma turbulence [13]. Refraction of the probe beam itself can be used as a diagnostic but even here the deviation of the light rays become too grotesque to handle. For example, for a parabolic density distribution $n_e = \hat{n}_e (1 - (r/R)^2)$, the angle of maximum refraction will occur at $r/R = 1/\sqrt{2}$ which, for ruby laser light ($\lambda_o = 6943$ Å), gives

$$\alpha_{max} = 4.3 \times 10^{-22} \, \hat{n}_e$$

Thus we have very large deflections, ~ 0.5 radians, even for $\hat{n}_e \sim 10^{21}$ cm^{-3}.

3. VERY HIGH DENSITY EFFECTS

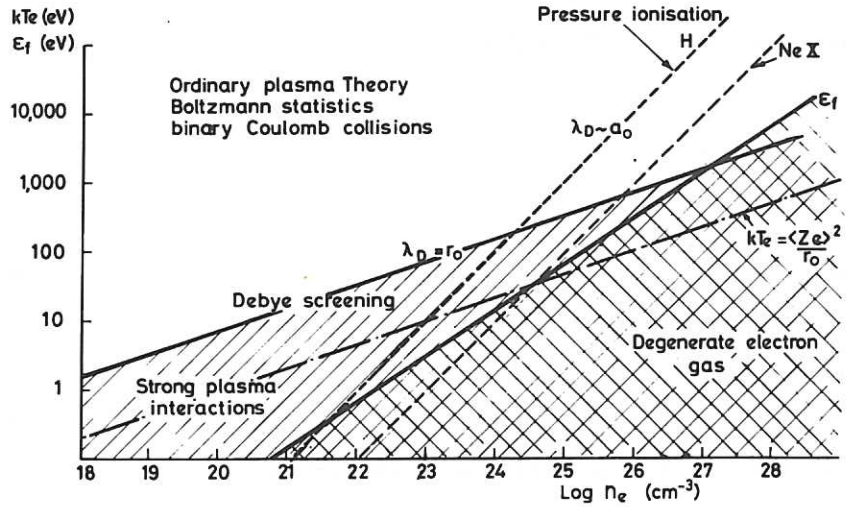

Figure 1
Schematic diagram of parameter space for conventional plasmas (upper left) and for regions where emission is modified by high density effects (lower right). Non-Debye plasmas (hatched area) has upper boundary given by equality of interparticle distance, r_o, and Debye length, λ_D; electron degeneracy (cross-hatched area) has an upper boundary defined by equality between the Fermi energy, ϵ_f, and the kinetic energy, kT_e.

The regions of parameter space where we expect modifications to the emission spectrum due to 'non-ideal' plasmas are shown in figure 1. Screening of the ion microfield by the electrons will become pronounced when the interparticle distance, r_o, is of the order of the Debye length λ_D, where $\lambda_D = V_{th}/(\sqrt{2}\ \omega_{pe})$. The number of particles in a Debye sphere is given by

$$n_D\ (cm^{-3}) = \frac{1.7 \times 10^9 T_e^{3/2}}{n_e^{\frac{1}{2}} (1 + Z)^{3/2}} \rightarrow 1.7 \times 10^9 . T_e^{3/2}\ (eV)\ n_e^{-\frac{1}{2}}\ (cm^{-3}) \quad \ldots (2)$$

; the latter expression being the more usual formula with the effect of the ion charges removed. It should be noted in (2) that screening is more sensitive to a lowering of T_e rather than an increase in n_e.

For $n_D \lesssim 1$, (hatched area in figure 1), Debye screening results in a splitting and shift of the energy levels towards the ionisation limit. Linear Stark theory may no longer hold in this region (section 5). Oscillator strengths and photoionisation cross sections are also altered [14]. The shape of the continuum intensity close to ω_{pe}, the plasma frequency, is affected [15] and the ionisation potential depressed [16]. Finally, non-linear coupling between

electron waves (plasmons) and the atomic levels can lead to induced, two-quantum transitions, (section 4).

Equating the lowering of the ionisation potential of an hydrogenic ion, charge state Z, to the potential energy in a bound state, with quantum level 'n', we have,

$$n_e \ (cm^{-3}) = 4.9 \times 10^{21} \ T_e \ (eV) \ Z^2 \ (1 + Z)^{-1} \ n^{-4} \qquad \ldots (3)$$

Pressure ionisation curves, using equation (3) are plotted in figure 1 for neutral H and Ne $\overline{X}$. These curves are illustrative rather than physically attainable since where they lie above the $\lambda_D = r_o$ boundary line, the inter-particle distance is already smaller than the radius of the first Bohr orbit, ie. $r_o < a_o$. The significance of the pressure ionisation curves below the $\lambda_D = r_o$ boundary is also doubtful since the concept of a Debye plasma is inherent in the derivation of equation (3). A lowering of the ionisation potential ($1 < n < \infty$ in equation (3)) is of course physically realisable and indeed is a common effect in high density plasmas.

The region of parameter space where correlations between particles become significant is shown, for Z = 1 in figure 1, as that area below the boundary line where their Coulomb energy $(Ze)^2/r_o$ is of the order of kT_e where r_o is now the ion interparticle distance. This occurs, for $n_z Z = n_e$, when

$$Z^5 \ n_e \ (cm^{-3}) = 1 \times 10^{20} \ T_e^{\ 3} \ (eV) \qquad \ldots (4)$$

At frequencies of the order of ω_{pe}, the continuum emission will be reduced by correlations due to the proximity of neighbouring ions. Due to the Z^5 dependence in equation (4), the strong plasma-interaction region in figure 1 can readily spill over to the upper "ordinary plasma theory" region in the case of highly-charged emitters. Correlations are shown to be important in line broadening studies, section 5.

At somewhat higher densities, failure of Boltzmann statistics occurs as the electrons become degenerate. The upper boundary is given by the condition that the electron Fermi energy, ε_F, equals kT_e, where,

$$\varepsilon_F \ (eV) = 1.5 \times 10^{-15} \ n_e^{\frac{2}{3}} \ (cm^{-3}) \qquad \ldots (5)$$

In future laser compression experiments, where densities which are orders of magnitude above the solid state may be reached, electron degeneracy will have the important effect of removing electrons from the free energy distribution. However in the present paper such extremes of density are not dealt with.

4. SATELLITE SPECTRA

The term 'satellite' is often used to describe emission features associated with, and having approximately the same energy as, a transition between two, well defined quantum states.

The physical processes leading to the appearance of satellite spectra can be quite separate and distinct however and, in order to avoid confusion, the features are often referred to as 'plasma' satellites, 'quasi-molecular' satellites or 'dielectronic' satellites etc. High pressure plasmas often by virtue of their non-stationary, non-thermal nature exhibit all three types of these features. The intensity and frequency of the satellites relative to the parent are the measurable quantities of interest and these can often be used as an estimate of the departure from a stationary ionisation balance and of the non-thermal content in the plasma sources.

(i) Plasma Satellites

Non-linear coupling between electro-magnetic fields and atomic systems, proportional to the square and higher orders of the electric field, has been known for many years as the AC Stark effect. In plasmas, electric fields of the same order as the Coulomb field in the plasma $E^2/8\pi \sim Ze^2/r$, can be imposed by intense beams of photons (transverse EM waves) or by plasmons (longitudinal plasma oscillations); sometimes even by a coupling between these two types of oscillations. The detailed theory [17] can be quite complex.

While plasma satellites are generally weak features relative to the allowed parent, the most likely features to be observed are those predicted by Baranger and Mozer [18] which occur in the vicinity of an optically forbidden transition with an allowed line situated nearby. A schematic term diagram of the forbidden line satellites is shown in figure 2.

If the pump field, intensity $\tilde{E}$ and frequency ω_{pe}, is sufficiently strong a two-quantum jump involving either 2 photons or a photon and a plasmon is predicted to occur at a separation from the allowed line given by $\Delta + \omega_{pe}$: where Δ is the frequency splitting between the forbidden and allowed lines. The upper level of the allowed line acts as a virtual state in the decay of the satellite levels, figure 2. In principle [18] the shape of the satellite line is determined by the energy spectrum of the plasma waves. Calculations of the interaction however, are generally based on linear, weak coupling theory which may be invalid in conditions of strong turbulence. Using a low density 'theta pinch' ($n_e \sim 5 \times 10^{13}$ cm^{-3}) Kunze and Griem [19] have reported satel-

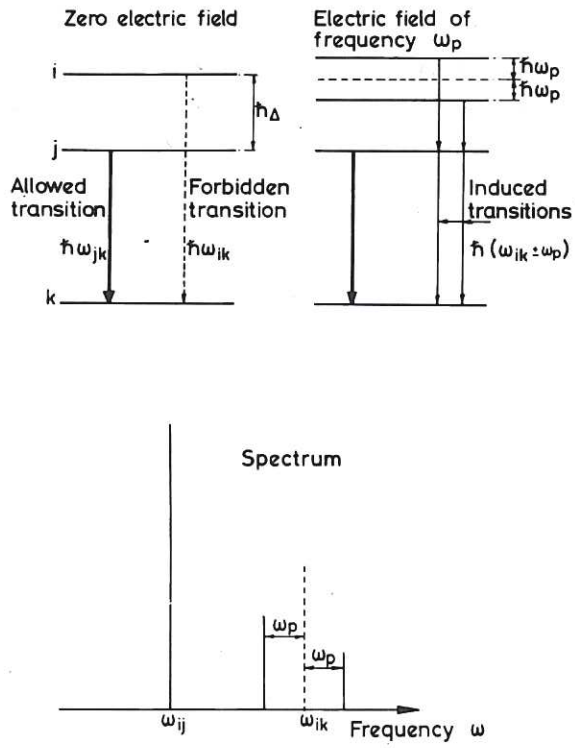

Figure 2
Schematic energy level diagram of induced satellites to a forbidden line.

lites to the 2p-nf forbidden transitions in He I and, following [18], derive values for the associated level of turbulence to be $\sim 10^3$ above the thermal level. Again at low density Cooper and Ringler [20] have successfully deduced the known transverse $\tilde{E}$ field in a microwave beam from the intensity of the induced satellites. Bekefi [15] gives a useful review of this relatively new field of optical transitions stimulated by plasma turbulence. Typically, the pump fields in these low density studies will be $\tilde{E} \sim$ kilovolts/cm or higher.

At higher densities, collective effects become more pronounced and may even be used, in certain circumstances, to measure the thermal level of the plasma waves. The ratio of the satellite to allowed line intensity [18] is given by

$$S_{\pm} = \epsilon \frac{kT_e}{4R_y} \cdot \left[\frac{\omega_{pe}}{\Delta \pm \omega_{pe}}\right]^2 \cdot R_{\ell\ell'} \qquad \ldots (6)$$

where $R_{\ell\ell'}$ is a dimensionless parameter [18] given in terms of the allowed $(m\ell)$ and forbidden $(m'\ell')$ quantum numbers, and ϵ is the ratio of the jitter energy of the electrons in the imposed plasma field to their thermal energy. For a thermal plasma and wave number $\overline{K}$,

$$\epsilon = \frac{4\pi \bar{K}_{max}^{3}}{3(2\pi)^3 \; 3n_e} = 0.015/n_D \qquad \ldots (7)$$

In equation (7) it is to be noted that as $n_D \rightarrow 1$, in high density plasmas with $kT_e > R_y$ (one Rydberg) thermally induced satellites can have measurable intensity. Plasma fields, $\tilde{E} \sim 2 \times 10^5$ V/cm, have been deduced [21] from the appearance of thermal plasma satellites.

More recently, and at much higher densities, satellites to the forbidden $1s^2\ {}^1S_0 - 1s\,2s\ {}^1S_1$, transition in He-like ions of the 3rd atomic period elements have been reported [22] in certain, laser-irradiated, target configurations. One line feature appears on the blue wing of the allowed $1s^2\ {}^1S_0 - 1s\,2p\ {}^1P_1$, line and is attributed to the anti-Stokes satellite to the forbidden line and separated from it by ω_{pe}. The density corresponding to this langmuir frequency is $n_e \sim 1 \times 10^{23}$ cm^{-3}. These observations [22] remain unconfirmed by independent measurements of the density, but point the way to a valuable new diagnostic in such extreme (8×10^7 atmospheres) plasma conditions.

At lower densities, the satellite, if due to plasma waves, would be immersed in the allowed line and this is perhaps the reason for its absence in plane target irradiation experiments, see figure 6, where the electron density is typically $\sim 10^{21}$ cm^{-3}.

(ii) Quasi-molecular Satellites

At very high densities as the ion separation becomes smaller it is possible for the ion perturber to form a quasi-molecule with the excited ion (emitter), the valency electron essentially being shared transiently between the two particles. The effect of proton perturbers, as calculated for Ly-α, [23], is to produce satellites in the wings of the transition at the energy separation corresponding to radii where the inter-atomic potential curves lie parallel. Satellite formation due to proton perturbers has been reported in the literature but perhaps the clearest evidence for quasi-molecular satellites comes from the effect of other ion perturbers, eg. Ar^+. In an argon arc plasma with $n_D \sim 1$ ($n_e = 2 \times 10^{17}$ cm^{-3}, $T_e = 1.4 \times 10^4$ ^{0}K) and lightly-doped with hydrogen, Preston [24] has shown that the far red wings of Ly-α display satellites, figure 3, whose intensity scales as the density product, $N(H, n = 2) \cdot N(Ar^+)$. The central frequency of these satellites is independent of T_e and n_e but the width weakly increases with T_e. Again, in a z-pinch plasma whose parameters are chosen so that $n_D \sim 1$, Baker [25] attributes the appearance of several satellites, displaced by up to 40 Å from line centre, as being due to

the formation of quasi-molecules such as (H, n = 2; Ar^+) and even (H, n = 2; Ar^{++}). One has to take cognisance of these quasi-molecular states in the interpretation of plasma parameters from satellite structure at high densities as described in 4 (iii).

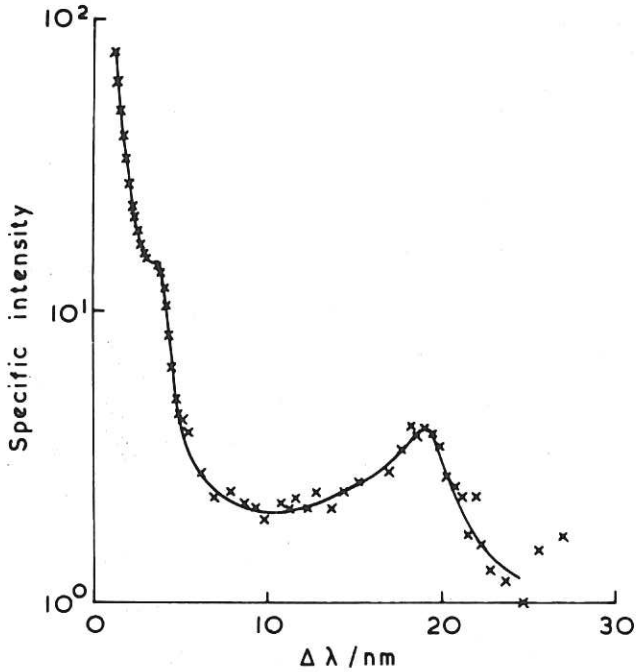

Figure 3
Logarithmic plot of the red wing of Ly-α in a hydrogen-doped, Ar arc. Two satellite features are observed, Preston [24].

(iii) Atomic Structure Satellites

Satellite spectra due to multiply-excited levels are common features of the XUV emission spectra from a wide range of plasma sources. In contrast to those discussed in 4 (i) and 4 (ii) their intensities can be comparable to the parent line. Satellite features were first reported by Édlen and Ťyren [26] who interpreted them as the parent transitions in the presence of an additional outer electron. For example, in the case of the first resonance line in H- and He-like ions we have respectively, 1s nℓ - 2p nℓ and $1s^2$ n'ℓ' - 1s 2 p n'ℓ' etc. Each of the higher members of the resonance series also have their associated satellite structure. This is shown in figure 4 for a laser-irradiated carbon target, the spectra from this source being remarkably similar to that in Édlen's original work [26].

In recent years, a great deal of term scheme analysis of multiply excited satellites has been carried out, see [27] [28] [29] [30]. The intensities of the satellites have been calculated in terms of collisional and radiative decay rates by Gabriel and others [28] [31] [32] [33] [34]. These calcula-

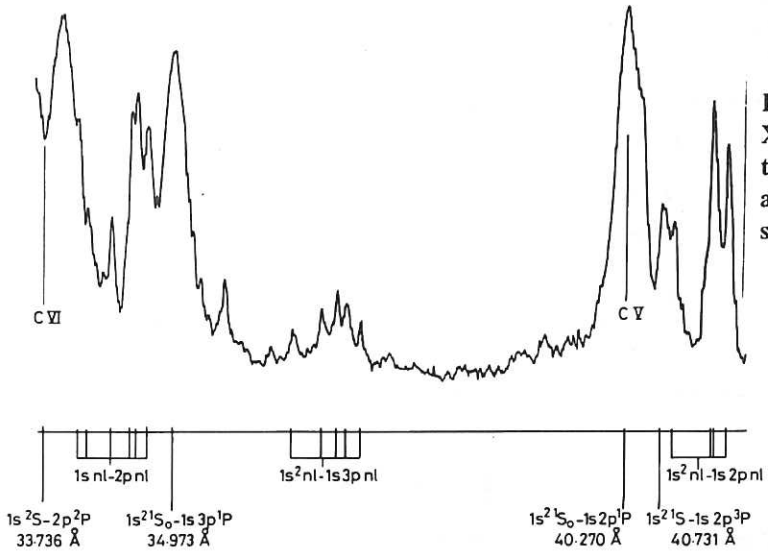

Figure 4
XUV spectrum of laser-irradiated $(CH_2)_n$ solid target. Satellite spectra to resonance lines of H- and He-like carbon are shown. Ly-α of CVI is self-reversed.

tions, as well as those pertaining to allowed and forbidden lines arising from radiative decay of 1s 2s $^3S_1$ and of 1s 2p $^3P_{210}$, form the framework for diagnostic measurements based on satellite lines of the He-like ions in high temperature plasmas.

The detailed appearance of the satellites changes with the relative rates at which their upper levels are populated and depopulated. Important among the populating processes are direct, inner shell excitation from the Li-like ion ground states and dielectronic recombination from the $1s^2\ ^1S$ + e, continuum. Dielectronic capture [35] followed by a stabilising radiative decay can be expressed quite generally by

$$e + X^{+Z}\ (n,\ell) \rightarrow X^{+(Z-1)}\ (n'\ell + 1;\ n''\ \ell'')$$
$$\rightarrow X^{+(Z-1)}\ (n\ell;\ \ n''\ \ell'') + h_u \qquad \ldots (8)$$

This process is illustrated in figure 5. Clearly, since there is exchange only between these electrons in the continuum with a specific energy E_s and the doubly excited bound state, energy E_e, the dielectronic process is temperature dependent (see also figure 8). Satellites, such as those arising from 1s $2p^2\ ^2P^e$ level, which for reasons of parity and angular momentum cannot couple via autoionising transitions to the continuum, are notably absent in recombining or steady state plasmas. The 1s $2p^2\ ^2P^e$ satellite is present only in strongly ionising plasma conditions. In view of these considerations it is a misnomer to refer to all transitions from multiply excited levels as

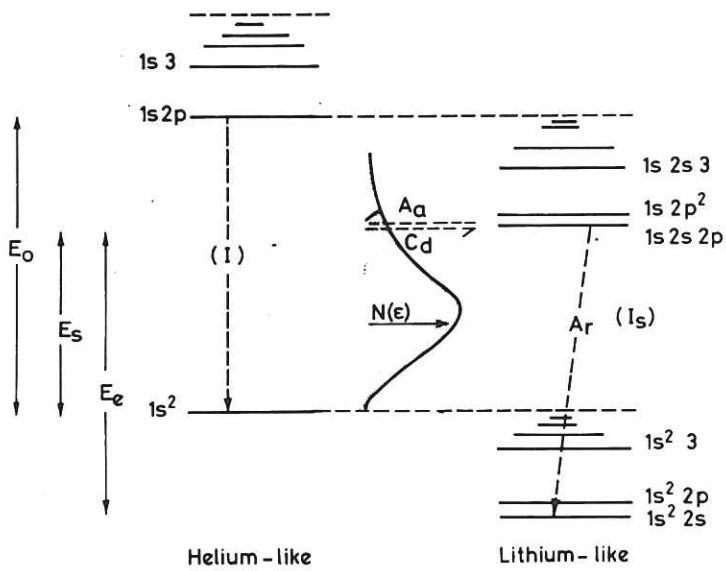

Figure 5
Schematic diagram of energy level structure of He-like ions and multiply-excited satellite levels of Li-like ions. The continuum electrons $N(\epsilon)$ recombine by dielectronic capture C_d, followed by stabilising decay A_r. A_a is the competing autoionising rate.

'dielectronic satellites'.

In high density plasmas such as those produced by laser-irradiation of solid targets, atomic structure satellites are intense features of the emission spectrum. The main contributions [36] come from $n' = 2$ and $6 > n'' > 3$ in equation (8) so that the satellites cluster around the first few resonance lines as illustrated for the Al ions in figure 6. The effect of high density is mainly a suppression of dielectronic recombination due to collisional ionisation of the upper levels [37]. Other, secondary and competing, effects of high density are stabilisation of the electron capture by collisional decay and the reversal of this process by possible reabsorption of the radiation under conditions of optical opacity. There are limits to the range of parameters over which temperatures can be derived from dielectronic satellites. For very highly charged ions, $Z > 17$ say, recombination tends to be dominated by collisional radiative effects. At very high densities $n_e > 10^{23}$ cm^{-3}, 3-body recombination becomes important.

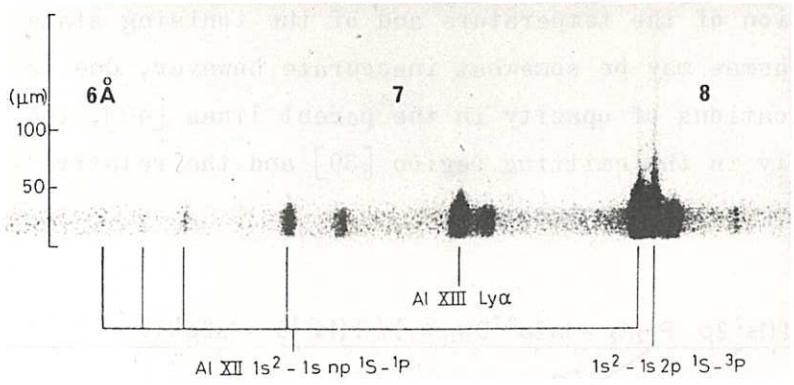

Figure 6
Space-resolved spectra from a laser-irradiated solid Al target. Satellites are clustered to the long wavelength side of the first resonance lines. Intensity of intercombination line ($^1S_0 - ^3P_1$) exceeds allowed line intensity in the recombining plasma $> 50\mu m$. Target surface is located at $0\mu m$.

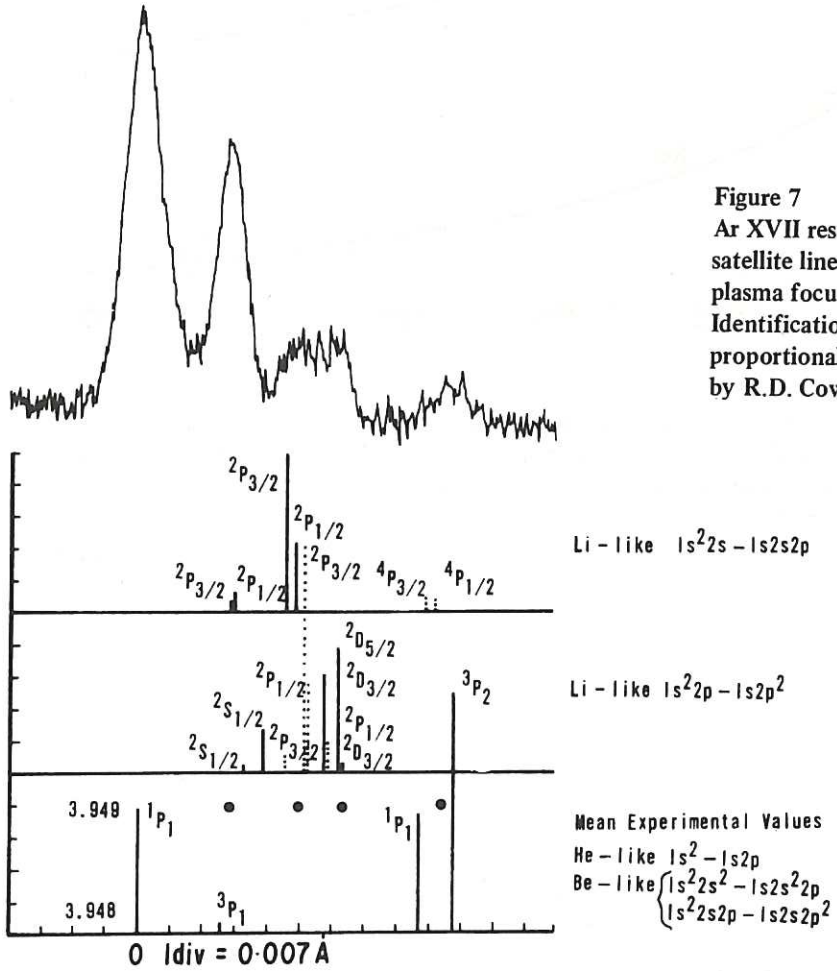

Figure 7
Ar XVII resonance line and associated satellite line structure emitted from plasma focus operated in D_2 + 5% Ar. Identifications (below) have intensities proportional to their gf values calculated by R.D. Cowan [43].

Several attempts have been made to derive the parameters of laser-irradiated solid targets from the relative intensities of the satellites, see eg. [33] [38] [39]. Derivation of the temperature and of the ionising state of these highly transient plasmas may be somewhat inaccurate however, due to the purely experimental complications of opacity in the parent lines [40], the sharp, spatial inhomogeneity in the emitting region [39] and the relative streaming velocities of different ion species [41].

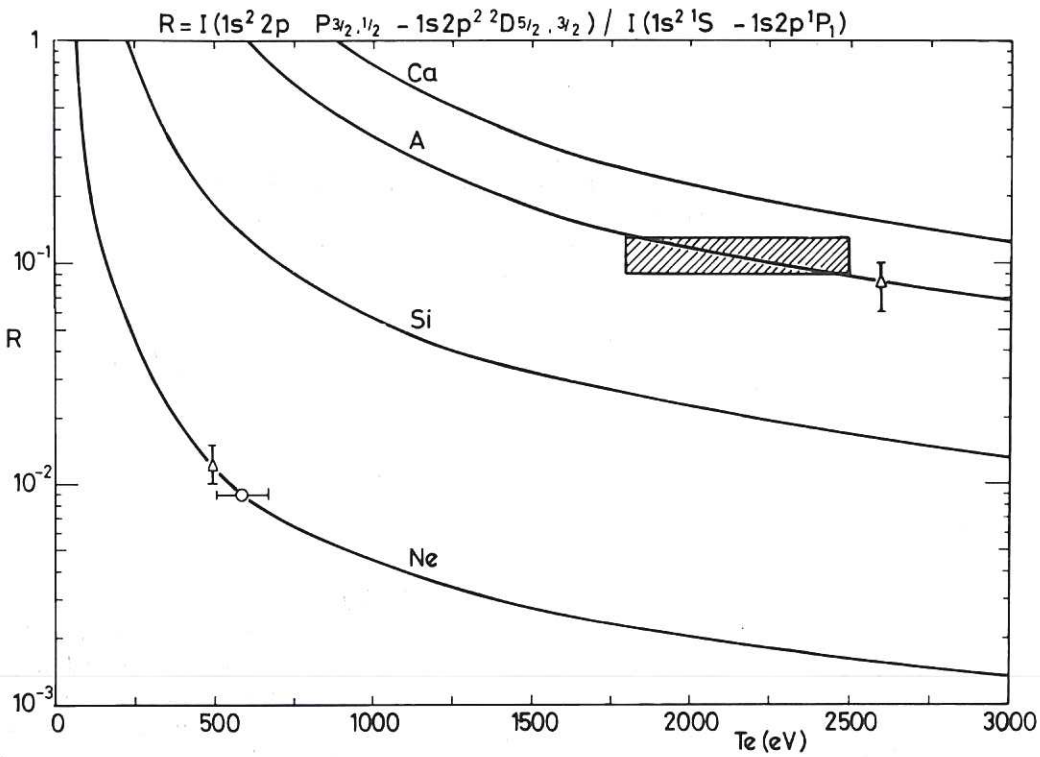

Figure 8
Intensity ratio of $1s2p^2\ ^2D$ satellites to $1s2p\ ^1P_1$ allowed line of He-like ions in the plasma focus. The Ar XVII values correspond to the plasma condition in Figure 7 while Ne IX corresponds to a gas filling of 0.5 torr Ne. In this latter case opacity in the allowed line is allowed for using the inter-combination line as an intermediate (optically thin) reference intensity. Full curves are theoretical predications of Gabriel [31]. Hatched area and ⊢o⊣ represent other experimental determinations of Te from the spectral intensity of the free-bound H-like ion continuum.

Screened transitions are prominent features in other high density sources including the low inductance vacuum spark and the plasma focus device. An example of satellite structure to Ar XVII in the dense plasma focus [42] is shown in figure 7. This source is relatively long-lived, a few tens of nanoseconds, with a density $n_e \gtrsim 10^{19}\ cm^{-3}$, and has been extensively diagnosed using several techniques including laser beam scattering. The Ar resonance

lines in this case are optically thin and the ion populations are consistent with mildly ionising conditions ie. approaching their steady-state values characteristic of the electron temperature which is the order of 2 keV. The satellite intensities should therefore provide a reasonable test of the theoretical models. It is interesting to note, figure 8, that the temperature derived from the satellite using Gabriel's model [31] is in good agreement with the value deduced by independent diagnostic methods.

5. LINE SHAPES AT VERY HIGH DENSITY

Pressure broadening of lines is widely used to estimate the density of plasmas. Almost all the experiments and theory, however, are appropriate to plasmas with density less than about 10^{19} particles cm^{-3} [44]. At much higher densities, lines in the visible region are often merged with continua emission so that one is compelled to study XUV emission, inevitably from multiply-ionised emitters. Theoretical estimates of line broadening for highly charged species, have not been adequately tested. One might expect, however, that effects of Debye screening of the ions, Coulomb repulsion between emitter and perturbers, perturber-perturber correlations and quadrupole effects become important for highly charged ions at densities much exceeding 10^{19} cm^{-3} [12].

Stark broadening of H-like ions causes much the most significant effect of density on line shapes and it is the most readily estimated. Vinogradov et al [12] point out that broadening of H-like ions will be quasi-static over a range of charge states from $Z = 1 \rightarrow 25$ and over a complementary range of density from $10^{18} \rightarrow 10^{23}$ cm^{-3}. Broadening by electrons which will affect mainly the line centre is due to impact mechanisms up to $n_e \sim 10^{25}$ cm^{-3}. An example of the ion broadened wings and electron-broadened core of CV1-Lγ is shown in figure 10.

There are two main corrections to the simple Holtsmark, quasi-static theory [44]. The first, which becomes important as $n_D \rightarrow 1$, is screening of the ions (both radiators and perturbers) by the electrons. This causes a reduction in the perturber ion microfield and therefore in the broadening. Corrections to the Holtsmark field have been considered in terms of the screening parameter $'a' = r_o/\lambda_D$ and the appropriate reduced fields have been tabulated [45]

$$'a' = r_o/\lambda_D = \frac{8.3 \times 10^{-4}\, n_e^{\frac{1}{2}}}{n_z^{\frac{1}{3}}\,(kTe)^{\frac{1}{2}}}, \qquad \ldots (9)$$

where kTe is in eV and r_o is the ion-ion separation.

Screening also gives rise to line shifts and asymmetries [46] the latter being due to Coulomb perturbations within the atomic structure of the radiating ion itself. The shift of the energy levels [12] towards the ionisation limit is given by

$$\Delta E_{n,\ell} = \frac{R_y}{2}\left(\frac{a_o}{\lambda_D}\right)^2 \cdot Z_{eff}^{\frac{1}{2}} \cdot \left[3n^2 - \ell(\ell + 1)\right] \qquad \ldots (10)$$

In the case of H-like ions, $\Delta E_{n\ell}$ is less than the Holtsmark line width while for non-hydrogenic ions in the range 10^{18} to 20^{24} cm^{-3} it is likely to be of the same order as the Doppler and impact widths.

A second correction to Holtsmark fields at high densities is required for correlations between particles, especially between emitters and perturbers. The criterion for correlations to be important is given in equation (4) and can be expressed as

$$Np \gtrsim \left[kTe/(Z - 1)\, Z_p e^2\right]^3 \qquad \ldots (11)$$

For plasma with a mean charge Z = 10 and kTe = 100 eV, for example, the perturber density $Np > 4 \times 10^{20}$ cm^{-3}. For highly charged ions $Z \gtrsim 10$, the range of Np where correlations are important is wider than that which leads to Inglis Teller line merging [44]. The effect of correlations on the whole line profile has been considered for the case of a two ion component plasma by O'Brien and Hooper [47]. Line shifts due to plasma polarisation effects have been predicted [44] when correlations are strong but so far they have proved illusive to measure [48].

Very few calculations exist for multiple component plasmas at high density; see however figure 10, in which O'Brien and Hooper's formalism [47] has been employed. The overall Stark broadening for H-like Al XIII, has been calculated [49] for densities in the range $10^{20} \lesssim n_e \lesssim 10^{24}$ cm^{-3}. Again, in a single ion component plasma the widths of Ly-α for ions of charge state Z can be estimated [50] as,

$$\Delta\omega_{\frac{1}{2}}\ (\text{keV}) = \frac{0.05}{Z}\ (5 \times 10^{22})^{\frac{2}{3}}$$

Calculations of the range of validity for simple but accurate modifications to Holtsmark fields experienced by H-like ions are shown in figure 9.

It is probably reasonable to assert that total line profiles, which are adequate for diagnostic purposes, can be constructed with reasonable accuracy from modified Holtsmark field distributions. Other corrections, especially to the line centres, are of secondary importance.

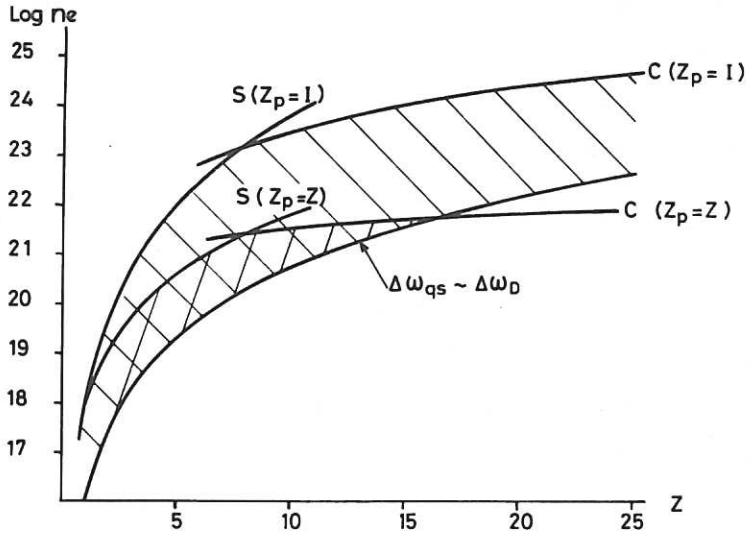

Figure 9
Hatched area shows range of density where simple modifications to Holtsmark fields give accurate line profiles for H-like ions with $Z = (kTe/Ry)^{1/2}$. The lower boundary is set by equality of quasi-static and Doppler half-widths. The upper boundaries 'S' correspond to a screening parameter 'a' = 0.2, for perturber charges Zp = I(\\\) and Zp = Z(///), where field may be readily interpolated by a suitable choice of reduced field parameter [51] from Hooper's tables [45]. Upper boundaries 'C' correspond to corrections of 10% to half-widths due to radiator-perturber correlations.

For non-hydrogenic lines Stark broadening is much smaller and impact effects are likely to govern the line widths for $n_e \lesssim 10^{24}$ cm^{-3}, the electrons and ions making equal contributions.

Experiments on line broadening at very high densities are still relatively uncommon. The CVI emission from laser-produced carbon plasmas has been studied however in recent years. Irons [52] measured the Stark broadening of high quantum number transitions in CVI, in the visible spectrum of laser-produced plasmas, in the case where $n_e < 3 \times 10^{18}$ cm^{-3}, $T_e < 30$ eV giving a screening parameter 'a' ~ 0.15. The half widths fitted reasonably well with the ion quasi-static estimates in which screening was taken into account, viz.

$$\Delta\omega_{\frac{1}{2}} \text{ (full half width)} = \frac{3}{2}\frac{\hbar}{meZ}\left(n_\ell + \tfrac{1}{2}\right) \times \overline{F}_o, \qquad \ldots (12)$$

where $\overline{F}_o = 8.8\, e\, Z_p^{\frac{1}{3}} N_e^{\frac{2}{3}}$; Z_p the mean charge of the perturbers. Aglitskii et al [53] using the (3-4) transition in CVI at 521 Å was able to estimate somewhat higher densities closer to the target surface.

In an earlier study of laser-irradiated solid targets, Burgess et al [54] attributed Stark broadening to the width of transitions in the region 100-200 Å from alkali ions of OVI and KIX. Simple estimates of the half widths due to

electron impact (straight, classical path) broadening gave electron densities which were self-consistent within a factor of 2. Ion broadening is not too important for these isolated non-hydrogenic lines and is in any case reduced still further due to Debye screening.

Broadening of the Lyman and Balmer series of CVI has been studied by Galanti et Al [40]. It appears that at densities $n_e \simeq 10^{21}$ cm^{-3} only a limited number of transitions in the series are relatively free from complications of line merging and optical opacity. Figure 10 shows the experimental profile of Ly - γ of CVI compared to the computed line shape. In these complex calculations [55] the ion-microfield due to the main perturbers, $N(C^{5+})$ and $N(6^{6+})$, has been corrected for the screening effect of the electrons using Hooper's formalism [47]. Electron collisions responsible for broadening in the core, are taken into account in the impact approximation. While the electron density derived from the Ly - γ profiles is consistent with that deduced from other spectroscopic features, these experiments [39] [40], can hardly be regarded as an adequate test of line broadening theory.

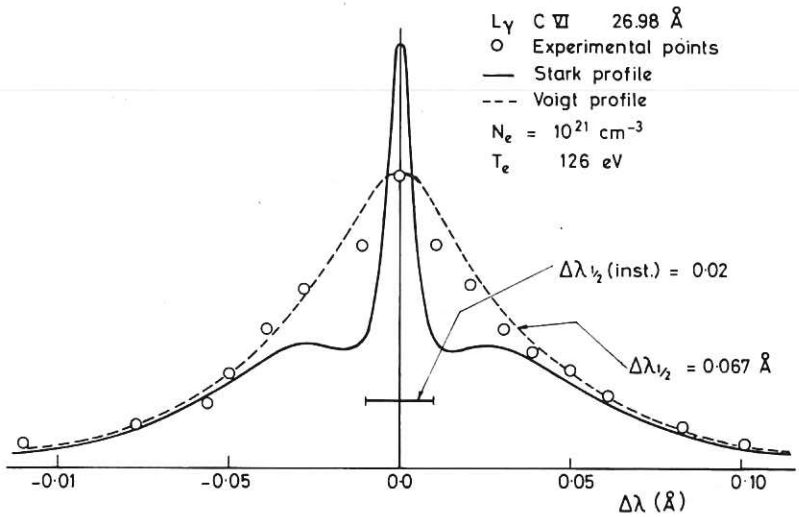

Figure 10
The full line is the Stark profile of CVI L_γ (26.98 Å) calculated [55] for a carbon plasma at 126 eV and an electron density of 10^{21} cm^{-3}. The Stark profile is folded with the instrument function to give the dotted line which is compared to the experimental profile represented by the circles.

6. OPACITY

Reabsorption of the emission, even in a homogeneous plasmas, can modify the spectral intensity of the source profile such that,

$$I(\nu) = S(T_e;\ n_e;\ Z)\ (1 - e^{-\tau(\nu)}) \qquad \ldots (13)$$

where $S(T_e;\ n_e;\ Z)$ is the source function which is determined essentially by ratio of the upper and lower state populations.

The optical depth $\tau(\nu)$ is given by

$$\tau(\nu) = N_\ell\ L(\nu)\ .\ \frac{h\nu_o}{C}\ .\ B_{12}\ .\ d \qquad \ldots (14)$$

N_ℓ is the number of atoms in the lower state of the transition, energy $h\nu_o$; and finally $L(\nu)$ is the absorption line shape within the plasma.

In the high density plasmas considered here $\tau(\nu)$ may greatly exceed unity for the first member of the resonance series. Since the plasmas are in general inhomogeneous and with streaming motion of the ions, [39] [41] [56], the effects of opacity on the core of the line can be very noticeable.
This is well illustrated in the spectra of CVI from a laser-produced target, figure 11. Lyman-α is clearly seen to be self-reversed, the core of the reversal progressively shifting to the blue wing of the profile as the plasma expands. The explanation can be understood by reference to the diagram in figure 12. Self-reversal can only occur if the source function $S(T_e,\ r)$ at the boundary of the plasma corresponds to a cooler T_e than that in the core, ie. $S(T_e;\ r) < S(T_e;\ o)$. In practice an adiabatic relation $T_e(r) = T_e(o)\ r^{-2(\gamma-1)}$ is often observed in those expanding plasmas.
Expressed as a function of the upper and lower level populations

$$\frac{n_2}{n_1}(r) < \frac{n_2}{n_1}(r = o)$$

If again, as has been observed [41], the streaming velocity $V(r)$ increases with distance from the target, ie. $V(r) = Kr$, then the centre of the absorption profile will always lie progressively further out from the line centre as the plasma expands away from the target, figure 12. Thus, independent of the direction of observation, one will, on this realistic model, always see a line assymmetry with a reversal, blue shifted by $\delta\omega_a \propto \delta V(r)$, figure 12. Clearly, measurement of the spatial variation of the blue shifted absorption region can be used to derive the functional relation $V(r) = Kr$. Appropriate model calculations of the dependence of emission line profiles on the source function and on plasma streaming have been constructed by Irons [57].

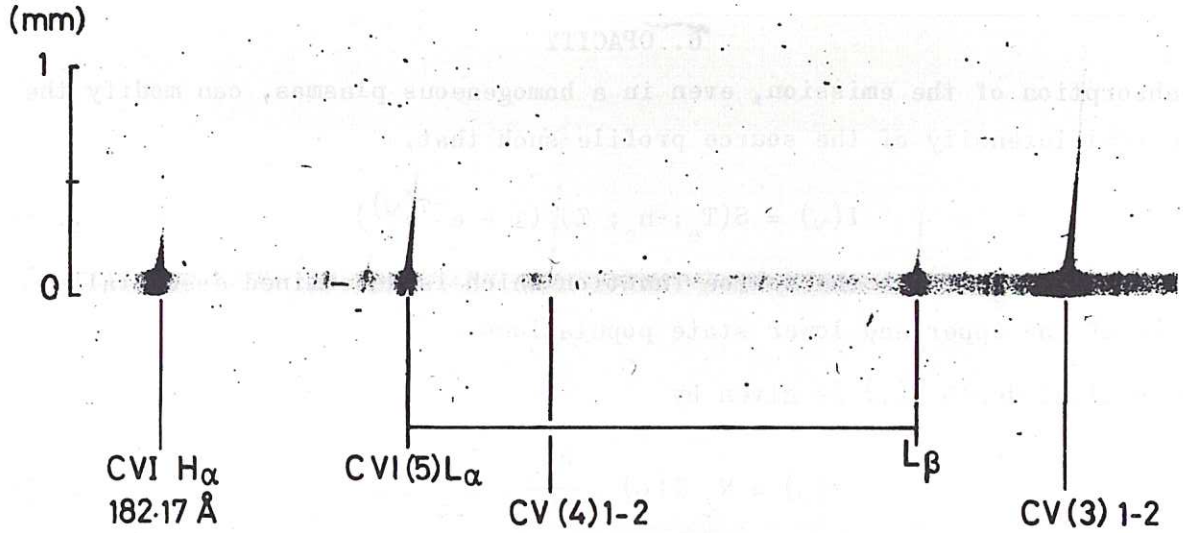

Figure 11
Space-resolved spectrum from laser-irradiated, solid $(CH_2)_n$ target, showing (in 5th and 6th order) the self-reversed and broadened lines of the CVI Lyman series. The cores of the absorption shift progressively to the blue wings with distance from the target surface.

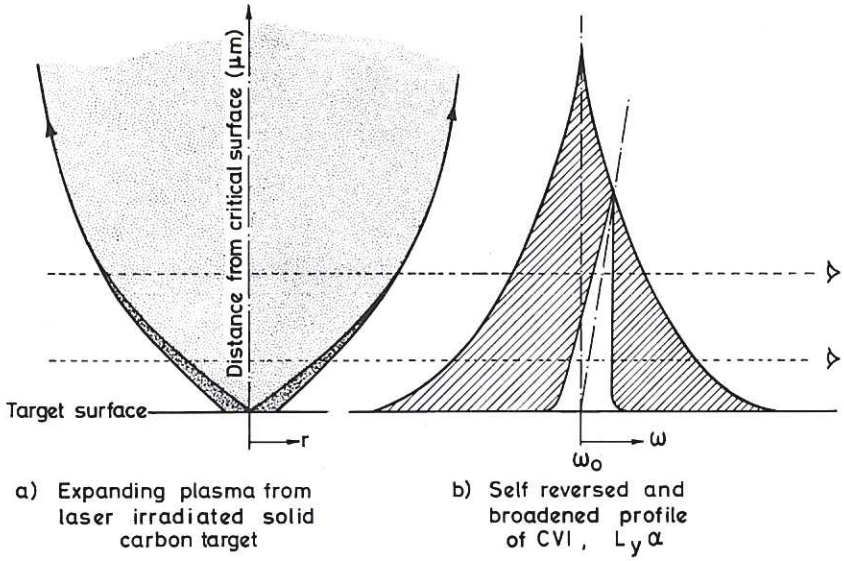

Figure 12
Model of plasma expansion (a); and of Stark broadened line profile in which self-reversal is shifted progressively to the blue wing as the plasma is viewed further from the target surface (b).

7. LINE INTENSITIES

The absolute intensity of an emission line may be used to derive either the temperature or the electron or ion concentration provided that a model can be constructed for the level populations in terms of collisional and radiative rate coefficients and provided that all of the other plasma parameters, including emission volume, are known. In the more usual case when a full

description of the plasma is not available it is more convenient to use intensity ratios of line belonging to the same ion. The ratio can generally be expressed as a function of only the radiative and collisional processes. In circumstances where these ratios are comparable, we have

$$n_e < \sigma v >^{coll}_{\ell u} \simeq A_{u\ell} \qquad \ldots (15)$$

and the model may be used to derive n_e. In other regions of parameter space the line ratio is only temperature dependent. Feldman and Doschek [58] have proposed a number of 'three level' atomic systems such as $2s^2\ 2p^q$, $2s\ 2p^{q+1}$, $2p^{q+2}$, in which two of the transitions are allowed and the third forbidden, then the ratio of the two allowed transitions is directly proportional to density. By varying the element and therefore the charge state Z for a fixed q, the range of n_e and T_e for which the measurements are valid, can be altered. Using equation (15) we have [58],

$$n_e \simeq \frac{6.1 \times 10^{22}\ \omega_\ell (T_e)^{\frac{1}{2}}}{(g)_{\ell u}\ \lambda^3\ \omega_u} \qquad \ldots (16)$$

Elements from Fe to Mo in the atomic table, with emission wavelengths from $2s\ 2p^{q+1}$ configurations which lie in the XUV region may be used to diagnose plasmas with a temperature of the order of 1 keV. For example, the intensity ratio of the multiplets $2s^2\ 2p^3 - 2s\ 2p^4/2s\ 2p^4 - 2p^5$ in FeXX with wavelengths $\simeq$ 110 Å, has been suggested [59] as a density monitor in the range $10^{16} < n_e < 10^{21}$ cm^{-3}. At still higher densities one is obliged to use shorter wavelengths, equation (16), and therefore more highly-stripped ion stages. In figure 8 we have illustrated temperature measurements using the intensities of the parent line of He-like ions and their associated satellite lines in the X-ray region. In H-like ions the complementary resonance and satellite line ratios have also proved useful [60]. The ratio of the inter-combination line to the resonance line in He-like ions has a convenient linearly-decreasing dependence on density over the limited range when, as in equation (15), $A(2^3P - 1^1S) \simeq n_e\ (\sigma(2^3 - 2^1)v)$. Densities $n_e \simeq 10^{19}$ cm^{-3}, have been determined in this way using Ne IX emission from the plasma focus [42] and at higher densities, $n_e \simeq 10^{22}$ cm^{-3}, Ar XVII has been proposed [61]. Presnyakov, [61], gives a useful summary of diagnostic experiments using He-like ions and their theoretical background.

Analysis based on models of line intensities commonly neglect optical opacity and assume that the internal relaxation times of the excited levels are shorter than the ion life time in a localised plasma region. Such approxi-

mations are not always valid for dense plasma sources and the simple models require a reconstruction to include complications such as non-stationary ion populations (as in figure 6) or opacity (section 6). It is clear that relative line intensities give a valuable indication of the equilibrium state of the plasma but the models should be used with caution in the evaluation of precise densities and temperatures. A line-broadening analysis section 5, is more appropriate for accurate values of the density.

Precisely because of the non-equilibrium conditions which can prevail in high energy-density sources it has for several years been speculated that these plasmas may be used for amplification of XUV light by stimulated emission. In the plasma expanding away from the surface of plane, laser-irradiated solid targets, population inversion has certainly been observed. But in this simple configuration the density of ions with inverted level populations is too low to observe gain, [62]. A number of suggestions have been made for increasing the inverted ion density including the use of other plasma sources in XUV optical pumping schemes, [63].

Until now, there have been several claims of marginal amplification by stimulated emission using the plasma as a gain medium, Jaeglé [64]. However these claims, in large part, rest on model calculations of radiative transfer through highly-transient, multi-component plasmas with inadequately known radiative and collisional rate coefficients. Clear experimental evidence for additional gain by stimulated emission, which can be quantitatively related to longer radiative path lengths in the plasma, is still lacking. A basic requirement for this is the use of more energetic primary laser systems. Lasers operating at 1 μm and 10 μm wavelengths with several kilojoules of energy in sub-nanosecond pulse durations are now available for material compression studies. Their application to gain experiments should result in rapid progress in XUV laser studies in the immediate future.

ACKNOWLEDGEMENTS

The author would like to thank D D Burgess and C C Smith of Imperial College, London, for useful discussions on this paper.

REFERENCES

[1] J. W. Mather Methods in Experimental Physics 9B, "Plasma Physics" Chapter 15 (Editors, R. H. Lovberg and H. R. Griem) Academic Press (1971)

[2] N. J. Peacock, M G Hobby and P. D. Morgan Proc. IVth Int. Conf. on Plasma Phys. and Controlled Nuclear Fusion Research, Madison U.S.A. (1971), Vol. 1, pp. 537-551, Published IAEA Vienna (1972)

[3] T. N. Lie and R. C. Elton Phys. Rev. A 3, pp. 865-871 (1971)

[4] J. L. Schwob and B. S. Fraenkel, Phys. Lett. 40, A. 1, pp. 81-85 (1972)

[5] E. Ya Golts, I. A. Zhitnik, E. Ya. Kononov, S. L. Mandelstam, Yn. V. Sidelnikov Report No. 4, Inst. of Spectroscopy, USSR Academy of Sciences (1974)

[6] M. H. Key, R. G. Evans et Al., "Implosion and Compression of Gas Filled Microballoons" Paper IV 9, 11th European Conf. on Laser Interaction with Matter, Oxford Sept. 1977. Rutherford Laboratory Report RL-77-122/B. Published by Science Research Council, U.K. (1977)

[7] J. Nuckolls, L. Wood, A. Thiessen and G. Zimmerman, Nature Vol. 239, pp. 139-142 (1972)

[8] R. W. P. McWhirter "Course on plasma diagnostics and data acquisition systems" (International School of plasma physics, Varenna) pp. 178-244 Published by Plasma Physics Laboratory CNR-Euratom, Milan. (Editors A. Eubank and E. Sindoni) (1975)

[9] C. Breton and J. L. Schwob "Vacuum Ultraviolet Radiation Physics" Chapter 8 "Vacuum ultraviolet emission from hot plasmas" pp. 241-284 (Damany, Vodar and Romand - Editors) Pergamon Press (1974)

[10] H. Conrads "Applied Spectroscopy Reviews", 6(2) pp. 135-188. Published by Marcel Dekker Inc. (1972)

[11] D. D. Burgess, Space Science Reviews 13 Nos. 4, 5 and 6, pp. 493-526 (1972)

[12] A. V. Vinogradov, I. I. Sobelman and E. A. Yukov, Kvant Electron (Mosc.) 1., pp. 268-278 (1974)

[13] V. A. Gribkov, O. N. Krokhin, G. V. Skliskov, N. V. Filippov and T. I. Filippova, VIth European Conf. on Controlled Fusion and Plasma Physics p. 375 Joint Inst. for Nuclear Research, Moscow (1973)

[14] B. F. Rozsnyai, Jnl. Quant. Spectrosc. and Radiative Transfer, Vol 17 pp. 77-88 (1976)

[15] G. Bekefi, "Comments on Plasma Physics and Controlled Fusion" 1, No. 1. pp. 9-16 Published by Gordon and Breach (London) (1972).

[16] H. R. Griem "Plasma Spectroscopy" McGraw-Hill, New York (1964)

[17] E. Courtens and A. Szöke, Phys. Rev, 15, No. 4 pp. 1588-1603 (1977)

[18] M. Baranger and B. Mozer, Phys. Rev. 123, 25 (1961)

[19] H. J. Kunze and H. R. Griem, Phys. Rev. Lett. 21, pp. 1048-1052 (1968).

[20] W. S. Cooper and H. Ringler, Phys. Rev. 179, pp. 226-236 (1969)

[21] B. Yaakobi and G. Bekefi, Phys. Letts. A. 30, pp. 539-540 (1969)

[22] V. A. Boika, O. N. Krokhin, S. A. Pikuz and A. Ya. Faenov, Zh. E.T.F. Pis Red. 20, pp.115-119 Transl. J.E.T.P. Lett., 20, No. 2 pp. 50-51 (1974)

[23] J. C. Stewart, J. M. Peak and J. Cooper, Astrophys. Jnl. 179, pp. 983-986 (1973)

[24] R. C. Preston, J. Phys. B. (Atom. Molec. Phys.) Vol 10, No. 3 pp. 523-540 (1977)

[25] E. A. M. Baker, "Spectral Line shapes in ultradense plasmas", PhD Thesis - University of London (1977)

[26] B. Edlen and F. Tyren, Nature 143, pp. 940 (1939)

[27] A. H. Gabriel and C Jordan, Nature 221, pp. 947-949 (1969)

[28] A. H. Gabriel and C. Jordan, "Case Studies in Atomic Collision Physics", Vol. 2, Chapt. 4 Editors McDaniel and McDowell, (Amsterdam: North Holland Publ. Co.) (1971)

[29] E. V. Aglitskii, V. A. Boika, S. M. Zakharov, S. A. Pikuz and A. Ya. Faenov, (a) Kvant. Electron 1, pp. 908-936 (1974) Transl. Sov. J. Quant. Electron. 4, No. 4 pp. 500-513 (1974) (b) ZH. E.T.F. Pis. Red. 19 No. 1 pp. 16-18 (1974)

[30] L. A. Vainstein and V. I. Safranova, (a) "Wavelengths and transitions probabilities for ions", Inst. of Spectroscopy, Moscow, Akademia Nauk. - USSR, Preprint No. 6 (1975)
(b) Preprint No. 146 Lebedev Inst. for Physical Sciences (1976)

[31] A. H. Gabriel, Mon. Not. Roy. Astron. Soc. 160, pp. 99-119 (1972)

[32] C. P. Bhalla, A. H. Gabriel and L. P. Presnyakov, Mon. Not. Roy. Astron. Soc. 172, pp. 359-375 (1975)

[33] E. V. Aglitski, V. A. Boiko, A. V. Vinogradov, E. A. Yukov, Kvant. Electron. (Mosc.) 1, pp. 579-590 (1974) Transl. Sov. J. Quant. Electron 4 No. 3 pp. 332-328 (1974)

[34] A. L. Mertz, R. D. Cowan, N. H. Magee, "The calculated power output from a thin Iron-seeded Plasma", L.A.S.L. Report - LA-6220-MS Published by Los Alamos Scientific Laboratory, USA (1976)

[35] A. Burgess, Astrophys. J. 139, pp. 776-780 (1964)
Astrophys. J. 141, pp. 1588-1590 (1965)

[36] T. P. Donaldson, "Dielectronic Recombination in Laser Generated Plasmas", Culham Lab. Report CLM-R 153. Available H.M. Stationery Office UK (1976).

[37] J. C. Weisheit, J. Phys. B. (Atom. and Molec. Phys.) 8, No. 15 pp. 2556-2564 (1975)

[38] U. Feldman, G. A. Doschek, D. J. Nagel, R. D. Cowan and R. R. Whitlock Astrophys. Jnl. 192, pp. 213-220 (1974)

[39] M. Galanti and N. J. Peacock, J. Phys. B. (Atom. Molec. Phys.) Vol 8, No. 14, pp. 2427-2446 (1975)

[40] M. Galanti, N. J. Peacock, B. A. Norton and J. Puric, Proc. Int. Conf. on Plasma Physics and Controlled Fusion (Tokyo) Proceedings series, Published IAEA (Vienna) Vol 2, pp. 405-419 (1974)

[41] F. E. Irons, R. W. P. McWhirter and N. J. Peacock, J. Phys. B. (Atom. Molec. Phys.) Vol 5, pp. 1975-1987 (1972)

[42] N. J. Peacock, "X-ray and Neutron Production Optimization in the Dense Plasma Focus" U.S.A.F. Report AFWL-TR-73-147 Published, Air-Force Systems Command, Kirtland AFB. New Mexico, USA (1973)
M. G. Hobby and N. J. Peacock, Proceedings of 10th Int. Conf. on Ionised Gases (Oxford), Published by Parsons & Co., Oxford (1971) pp. 407 (1971)

[43] R. D. Cowan, Phys. Rev. 163 pp. 54-61 (1967) Private Communication (1969)

[44] H. R. Griem, "Spectral Line Broadening in Plasmas", Published by Academic Press (New York and London) (1974)

[45] C. F. Hooper, Phys. Rev. 165, pp. 215-222
Phys. Rev. 169, pp. 193-195 (1968)

[46] J. C. Weisheit and B. F. Rozsnyai, J. Phys. B. (Atom. Molec. Phys.) Vol 9, No. 4 pp. L63-67 (1976)

[47] J. T. O'Brien and C. F. Hooper, Phys. Rev. A. 5, pp. 867-884 (1972)

[48] D. D. Burgess and N. J. Peacock, J. Phys. B. (Atom. Molec. Phys.) 4, pp. L94-97 (1971)

[49] P. C. Kepple and H. R. Griem, N.R.L. Memorandum Report 3382, Naval Research Laboratory, Washington D.C. (1976)

[50] G. F. Chapline, H. E. Dewitt and C. F. Hooper, UCRL Preprint No. 46272 Lawrence Livermore Laboratory, U. of California (1974)

[51] C. C. Smith and N. J. Peacock, Culham Laboratory report (1977)

[52] F. E. Irons, J. Phys. B. (Atom. Molec. Phys.) 6, pp. 1562-2581 (1973)

[53] E. V. Aglitskii, V. A. Boika, S. M. Zahkarov and G. V. Sklizkov, Lebedev Institute Report No. 143 (1970)

[54] D. D. Burgess, B. C. Fawcett and N. J. Peacock, Proc. Phys. Soc. 92, pp. 805-816 (1967)

[55] A. G. Richards - Private Communication. Imperial College, (1974)

[56] N. J. Peacock, "Beam-Foil Spectroscopy" Vol 2, pp. 925-950 Plenum Publishing Corp. New York (1976)

[57] F. E. Irons, J. Phys. B. (Atom. Molec. Phys.) Vol 8, No. 18 pp. 3044-3068 (1975) Ibid. Vol 9, No. 15, pp. 2737-2753 (1976)

[58] U. Feldman and G. A. Doschek, Jnl. Opt. Soc. Am. 67, No. 6, pp. 726-734 (1977)

[59] G. A. Doschek, U. Feldman, J. Davis and R. D. Cowan, Phys. Rev. A. 12, No. 3, pp. 980-986 (1975)

[60] V. A. Boika, S. A. Pikuz, U. I. Safranova and A. Ya. Faenov, Kvantovaya Electron (Moscow) 4, pp. 600-606 (1977). Transl. Sov. J. Quant. Electron 7, No. 3 pp. 333-336 (1977)

[61] L. P. Presnyakov, Usp. Fiz. Nauk. 119, pp. 49-73 (1976) Transl. Sov. Phys. Usp. 19, No. 5 pp. 387-399 (1976)

[62] F. E. Irons and N J. Peacock, J. Phys. B. (Atom. Molec. Phys.) 7, pp. 2084-2099 (1974)

[63] B. A. Norton and N..J. Peacock, J. Phys. B. (Atom. Molec. Phys.) Vol 8, No. 6 pp. 989-996 (1975)

[64] P. Jaeglé, Proc. XIIIth Int. Conf. on Phenomena in Ionised Gases (Berlin G.D.R. September 1977), Invited Papers - Vol. 3 (1977).